

See discussions, stats, and author profiles for this publication at: <https://www.researchgate.net/publication/236124120>

Molecular Structure of 3-Aminopropyltriethoxysilane Layers Formed on Silanol-Terminated Silicon Surfaces

ARTICLE in THE JOURNAL OF PHYSICAL CHEMISTRY C · FEBRUARY 2012

Impact Factor: 4.77 · DOI: 10.1021/jp212056s

CITATIONS

44

READS

795

7 AUTHORS, INCLUDING:



Amanda V Ellis

Flinders University

147 PUBLICATIONS 1,925 CITATIONS

SEE PROFILE



Claire E Lenehan

Flinders University

61 PUBLICATIONS 692 CITATIONS

SEE PROFILE



Dmitriy Khodakov

Rice University

25 PUBLICATIONS 204 CITATIONS

SEE PROFILE



Gunther G Andersson

Flinders University

80 PUBLICATIONS 813 CITATIONS

SEE PROFILE

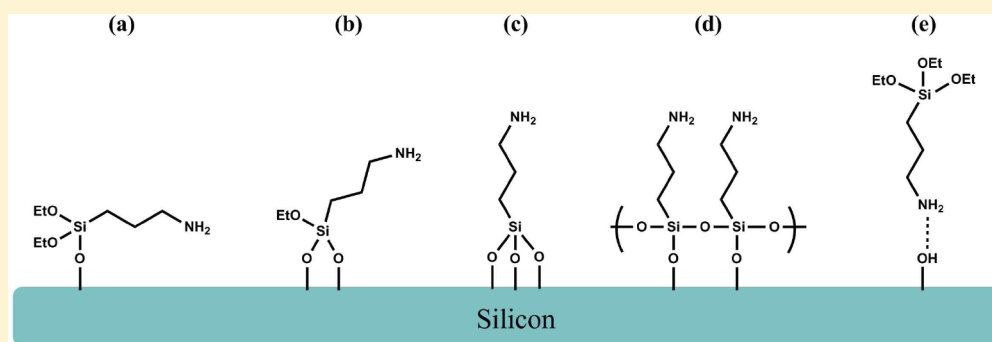
Molecular Structure of 3-Aminopropyltriethoxysilane Layers Formed on Silanol-Terminated Silicon Surfaces

Robert G. Acres,[†] Amanda V. Ellis,[†] Jason Alvino,[‡] Claire E. Lenahan,[§] Dmitriy A. Khodakov,[†] Gregory F. Metha,[‡] and Gunther G. Andersson^{*,†}

[†]Flinders Centre for NanoScale Science and Technology, Flinders University, P.O. Box 2100, Adelaide, SA 5001, Australia

[‡]School of Chemistry and Physics, University of Adelaide, 5005 Australia

[§]School of Chemical and Physical Sciences, Flinders University, P.O. Box 2100, Adelaide, SA 5001, Australia



ABSTRACT: The use of the coupling agent, 3-aminopropyltriethoxysilane (APTES), in the silanization reaction with silanol-terminated silicon is an important surface modification reaction. Of particular importance is that the terminal amine functionalities of APTES are sufficiently exposed to the gas or liquid phase for further modifications, such as amide coupling reactions. Here, metastable induced electron spectroscopy (MIES) and UV photoelectron spectroscopy (UPS) were used to study the composition of the outermost layer of a silanol-terminated Si surface after silanization with APTES. High-resolution X-ray photoelectron spectroscopy (XPS) was used to validate the attachment of APTES to the surface. Density of States (DOS) calculations were employed for interpreting the MIE spectra. Findings showed that amine functionalities covered only a small fraction of the APTES-modified Si surface.

INTRODUCTION

Alkoxysilanes are frequently used as coupling agents for attaching organic molecules to hydroxylated glass or silicon dioxide substrates.¹ The choice of alkoxysilane can influence the properties of the organic layer being attached, such as its density and the orientation of molecules within the layer. A popular choice of coupling agent is 3-aminopropyltriethoxysilane (APTES) as it allows for further attachment of molecules through its terminal amines and also exhibits self-assembly.^{1,2} Silanization is most often used to attach APTES onto various surfaces.³ This reaction involves the initial hydroxylation of silicon dioxide or glass with subsequent hydrolysis of the APTES ethoxy groups with ethanol as the leaving group, resulting in an aminopropyl-terminated surface (see Figure 1).² The type of solvent strongly affects the density and conformation of the covalently attached APTES layer.⁴ APTES forms an internal zwitterion in water, and therefore anhydrous solvent is used to produce a more uniform monolayer deposition. In such a configuration, the amine group is pointing away from the solid sample, thus pointing toward the liquid or gas phase, leaving free amine groups available for further functionalization.⁴

However, obtaining a uniform monolayer with the amine groups orientated away from the underlying substrate can be a complex issue, as APTES is very sensitive to a number of reaction conditions.^{2,5} Horizontal polymerization can occur when ethoxy groups are hydrolyzed due to water present in the system. The resulting silanol moieties can then react with each other via a condensation reaction to produce siloxane bonds. Vertical multilayering can also occur when APTES molecules physisorb to each other on an already APTES-treated surface.⁵

Amines are known to be hygroscopic, and therefore even with anhydrous solvent, trace amounts of water will be adsorbed.⁶ Chiang et al.⁴ have shown that the conformation of APTES differs between samples that have been air-dried, compared with those that have been heat-cured in an oven. It was found that air-dried APTES forms one or two siloxane bonds on the glass surface, whereas heat-cured APTES tends to form three siloxane bonds with the surface.⁴ Oven curing also helps to remove surplus solvent.⁷ In addition to solvent choice and curing methods, other reaction conditions can affect the

Received: December 14, 2011

Revised: January 27, 2012

Published: February 1, 2012



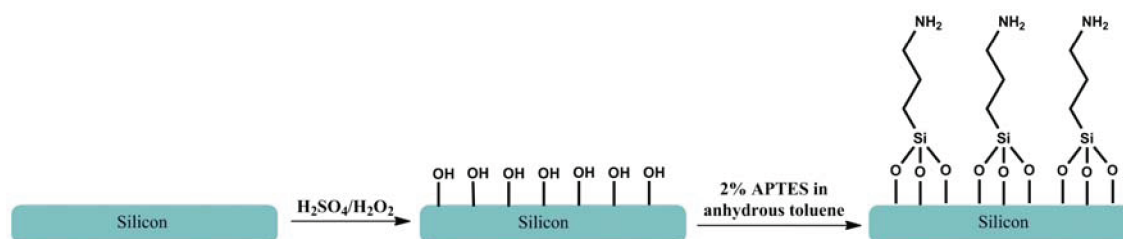


Figure 1. Hydroxylation of silicon, silicon dioxide, or glass with 3:1 $\text{H}_2\text{SO}_4/\text{H}_2\text{O}_2$ solution, followed by a silanization reaction between APTES and the hydroxylated surface giving rise to a proposed APTES functionalized surface. The terminal amine groups allow further functionalization.

structure and orientation of APTES. Vandenberg et al.⁵ found the average density of the APTES coverage always increased with increasing reaction time. APTES deposited from anhydrous toluene was found to produce nearly a monolayer on the surface (0.7 nm) when the reaction was kept to less than one hour, with the optimal time being 20 min.⁵ Longer silanization times cause the APTES molecules to polymerize, resulting in multiple layers and nonuniform coverage.⁸

Studies relating to APTES monolayer density on glass surfaces have shown that APTES had on average between 2.1 and 4.2 amine groups per square nanometer.^{9,10} This was measured by reacting the aminosilane with anthracenecarboxaldehyde to form an imine that was hydrolyzed in a known volume of water and its absorbance determined using UV–visible spectroscopy.^{9,10} Han et al.¹¹ immersed substrates into 5% (v/v) APTES/ethanol and heated them at 50 °C for between 20 min and 20 h, resulting in nonuniform layers, measured by ellipsometry. Layer thicknesses ranged from 10 to 140 nm implying that APTES can form thicker layers under certain conditions.¹¹ The concentration of APTES in anhydrous toluene is another factor that must be taken into account. Wang et al.¹² performed optimization studies using concentrations ranging from 1% to 10% and found 2% to be the optimum concentration for further functionalization. APTES has also been shown to remain stable, with Herlem et al.¹³ reporting that after one month APTES had remained stable on a Au(111) substrate, showing no sign of cracking or flaking. This was measured using ellipsometry in a clean room over one month to detect changes on the surface.

Obtaining the right structure and density of the aminosilane layer with terminal amines in the outermost layer is very important with regard to subsequent surface modifications. Vandenberg et al.⁵ studied the structure of APTES on silicon oxide substrates using X-ray photoelectron spectroscopy (XPS), atomic force microscopy (AFM), ellipsometry, and scanning electron microscopy (SEM) and observed that the surface amine groups were present in two forms, a “free” NH_2 that did not exhibit any binding to neighboring molecules and also NH_2 that was either protonated or hydrogen bonded. This study also showed that in many cases the APTES layers were only partially covalently bonded or hydrolyzed, with some APTES molecules retaining their ethoxy groups.⁵

In summary, several analysis methods have been employed to study the morphology and chemistry of APTES surfaces, including ellipsometry, XPS, and UV–visible, and infrared (IR) spectroscopies. These studies have shown much regarding the structure of APTES, such as horizontal polymerization, the presence of ethoxy groups after silanization, and the stability of APTES films over time. However, all these techniques do not provide monolayer surface-sensitive chemical analysis for the conclusive characterization of the terminal functionality of the

monolayer. Thus, applying methods sensitive exclusively for the outermost layer for analyzing the surface of APTES-modified surfaces is a crucial prerequisite for optimizing the surface density of the NH_2 groups, i.e., the functional groups allowing the APTES layer to function as an active layer for further coupling reactions.

Metastable induced electron spectroscopy (MIES) is capable of determining the composition of the outermost layer of a sample.^{14–19} MIES uses metastable helium atoms to induce electron emission from a surface, resulting in valence band spectra similar to ultraviolet photoelectron spectroscopy (UPS). Apart from the orbitals in the helium atom, only electron orbitals located in the outermost layer of the sample are involved in the de-excitation process of the metastable helium atoms. The sensitivity of MIES exclusively for the outermost layer makes the method useful for probing the functionality of an APTES-modified surface.

The aim of this study is to use a combination of MIES and XPS to analyze the nature of the outermost layer of APTES deposited onto a silanol-terminated silicon wafer. MIES was used to determine the density and character of available functional groups on the surface. The APTES layer subsequently shall later be used as a coupling layer for the attachment of further molecules which is beyond the scope of the present paper.

MIE reference spectra have been measured using chemical vapor deposited (CVD) layers of APTES on silver. Density of States (DOS) calculations of APTES were performed and used in conjunction with the reference spectra to interpret the MIE and UP spectra from APTES deposited on silanol-terminated silicon.

■ EXPERIMENTAL SECTION

Sample Preparation. *Silanol-Terminated Silicon Substrates.* Silicon wafers (nonporous, polished silicon (100) wafers (p++ type, boron doped, 0.0008–0.0012 Ω cm), Siltronic, France) were cut into squares (1–2 cm^2) and immersed in acetone and ultrasonicated for 30 min to remove surface contaminants. The Si substrates were then rinsed with deionized water, dried under a stream of nitrogen, and placed in a piranha solution (conc. $\text{H}_2\text{SO}_4/\text{H}_2\text{O}_2$ (2.5:1 v/v) for 30 min at room temperature, resulting in silanol-terminated Si surfaces. Subsequently, the samples were washed with deionized water and dried under a stream of nitrogen.

APTES Modification of Silanol-Terminated Silicon Substrates. Immediately following the piranha treatment, the dried silanol-terminated Si substrates were immersed in a freshly prepared solution of APTES (Sigma Aldrich, Australia) and anhydrous toluene (2% (v/v) APTES) for 20 min at room temperature, followed by thorough rinsing with anhydrous toluene to remove any excess reagent. Finally, the APTES-

modified Si substrates were heated in an oven at 110 °C for 20 min and then stored in a desiccator under vacuum until further use.

APTES Reference Sample. A reference sample of APTES was prepared by CVD on polycrystalline silver (99.99% purity). To perform the CVD deposition, the silver substrate was cooled to 90 K on a solid sample stage, and a stream of APTES gas was directed onto the silver substrate through a capillary positioned approximately 1 cm above the silver substrate. The stream of the gaseous APTES was controlled with a dosing valve. Prior to dosing, the APTES was degassed by gentle heating to remove air from the gas supply system.

Electron Spectroscopy. Investigations of the samples with XPS, MIES, and UPS were performed in an ultrahigh vacuum (UHV) apparatus built by SPECS (Berlin, Germany). The apparatus is equipped with a two-stage cold cathode gas discharge from MFS (Clausthal-Zellerfeld, Germany) to simultaneously generate metastable helium atoms ($\text{He}^* \text{ } ^3\text{S}_1$) and UV light (He I line) and a nonmonochromatic X-ray source for Mg and Al $K\alpha$ radiation. The spectra of the electrons emitted from the samples are recorded with a hemispherical Phoibos 100 energy analyzer from SPECS. MIE and UP spectra were recorded at a pass energy of 10 eV. At this pass energy the analyzer has an energy resolution of 400 meV as evaluated from the Fermi edge of polycrystalline silver. High-resolution XP spectra were collected using a pass energy of 10 eV for C 1s and Si 2p and 20 eV for N 1s. The apparatus is further equipped with an ion source for rare gas ions with kinetic energy from 1 to 5 keV. The angles between the He^*/UV light irradiation and the analyzer and the X-ray irradiation and the analyzer are both 54°. The base pressure of the UHV chamber was a few 10^{-10} mbar, although UHV conditions are not required for the experiments shown here.

High-resolution XP spectra were fitted using combined Gaussian–Lorentzian peaks with background correction using the Shirley method.²⁰ MIE and UP spectra were fitted with Gaussian curves and an exponential curve for the secondary electron background.²¹ In electron spectroscopy, secondary electrons are generated when electrons are inelastically scattered. These secondary electrons then can excite additional secondary electrons in a cascading process that produces a background signal in the measured spectrum, the shape of which can be approximated using an exponential function.²² The exact shape of the secondary electron background, however, is of minor importance for our analysis, as in the energy range which we will consider below the secondary electron background is considerably smaller than the intensity of those emitted electrons which do not experience inelastic scattering processes.

In a UPS experiment, the sample is irradiated with UV photons, leading to photoionization via the photoelectric effect. The energy of emitted electrons is given by

$$E_{\text{kin,h}\nu} = E(h\nu) - E_{\text{bin}} \quad (1)$$

where $E_{\text{kin,h}\nu}$ is the kinetic energy of the emitted electron, $E(h\nu)$ the photon energy (21.2 eV for the HeI line used here), and E_{bin} the binding energy of the electron before excitation. With UPS the electron density in the near-surface area is measured since the probing depth is limited by the electron mean free path of the emitted electrons. At the excitation energy used in this study, the electron mean free path in organic compounds is around 10–20 Å.²³ For the XPS experiment, an excitation energy of 1253.6 eV (Mg $K\alpha$) was used. For XPS the same

relation between kinetic energy of the emitted electrons, excitation energy, and the binding energy holds as for UPS. The methods differ, however, in their probing depth.

In a MIES experiment, the sample is irradiated with He^* atoms which are de-excited at the surface either via Auger de-excitation or via resonant ionization with subsequent Auger neutralization.^{14,15} The first process applies, in particular, for organic materials and semiconductors and thus applies in the present case. Resonant ionization is only possible for materials with an unoccupied surface orbital in resonance with the 2s orbital of the impinging He^* atom, e.g., for metal surfaces with a high work function. The electronic energy of the helium atom is transferred to the sample surface leading to the excitation and emission of electrons in the sample. The energy of the emitted electrons is given by

$$E_{\text{kin,He}^*} = E(\text{He}^*) - E_{\text{bin}} \quad (2)$$

where $E_{\text{kin,He}^*}$ is the kinetic energy of the emitted electron, $E(\text{He}^*)$ the excitation energy of the He^* atoms, and E_{bin} the binding energy of the electron before excitation. The majority of He^* atoms emitted from the UV/ He^* source is in the $^3\text{S}_1$ state which has an excitation energy of 19.8 eV. Due to the large cross section for the de-excitation processes, the He^* reacts with the sample at a distance of a few angstroms to the surface.^{14,15} For this reason, MIES is only sensitive to the electronic structure of the outermost layer.

DOS Calculations. For DOS calculations, geometry optimizations were performed using density functional theory in the Gaussian 09 suite of programs.²⁴ Calculations were performed using the B3LYP functional with Dunning's aug-cc-pVTZ basis set. All isomers underwent vibrational frequency calculations to ensure that the optimized structure was a true minimum. The lowest-energy structural isomers were used to produce the predicted DOS using the GaussSum software suite.²⁵

The UP and MIE spectra were fitted with Gaussian curves where in each case only the minimum number of Gaussian curves was used to fit a spectrum. The fitted peaks represent an electron orbital or DOS with a specific binding energy. The full-width-half-maximum (fwhm) is a fitting parameter since it is influenced by a number of factors. In general, the minimum fwhm is given by the natural line width of a peak, the resolution of the spectrometer, and the energy distribution of the excitation energy. Condensed phase spectral peaks are broader than peaks of the same substance in the gas phase due to interaction between the atoms or molecules in the condensed phase.²⁶ In the present case, the fwhm of the fitted peaks is also influenced by the fact that a single fitted peak represents more than a single DOS and needs to be considered as the sum of Gaussian functions where each one represents a single DOS. As a consequence, the fwhm of the fitted peaks is also influenced by the energy range over which the DOS are distributed. As the range covered by each fitted peak varies, the fitted peaks also differ in their fwhm. The calculated DOS were used to identify the nature of the peaks fitted to the measured spectra. An offset of 1.8 eV was added to the binding energy of the calculated spectra to account for the shift in electronic state energies that occurs between the gas and condensed phases. This adjustment of the binding energies has to be considered as the DOS calculations represent an isolated molecule in the gas phase.

RESULTS AND DISCUSSION

XPS Analysis of an APTES-Modified Si Substrate. XPS analysis was conducted to monitor each step of the attachment of the APTES layer onto the silanol-terminated Si wafer. Figure 2A shows the high-resolution C 1s spectrum of the silanol-

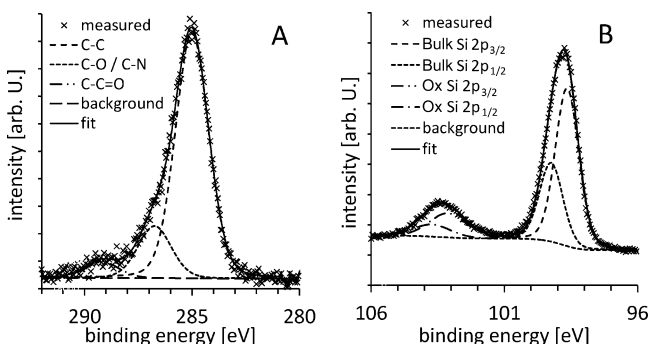


Figure 2. High-resolution XP spectra from silanol-terminated Si wafers. (A) C 1s and (B) Si 2p.

terminated Si wafer, indicating the presence of hydrocarbon contamination on the surface.²⁵ Presented alongside the C 1s spectrum in Figure 2B is the Si 2p XPS spectrum of the silanol-terminated Si wafer. Two distinct doublets were observed, corresponding to bulk silicon (98.7 eV) and silicon bonded to oxygen (103.1 eV).²⁷ Quantification of these high-resolution spectra is presented in Table 1 and Table 2.

Table 1. Quantification of the C 1s XP Spectrum in Figure 2A

species	position (eV)	contribution (%)
C–C	285	78 ± 1
C–O/C–N	286.7 ± 0.2	17 ± 1
C–C=O	289.2 ± 0.3	5 ± 1

Table 2. Quantification of the Si 2p XP Spectrum in Figure 2B^a

species	position (eV)	contribution (%)
bulk Si	98.7 ± 0.1	80 ± 0.5
native SiO ₂	103.7 ± 0.1	20 ± 0.5

^aThe position of the Si 2p 3/2 peak is shown.

High-resolution XP spectra from an APTES-modified Si wafer are presented in Figure 3. The C 1s spectrum in Figure 3A shows all the functionality that would be expected from

APTES, namely, C–C at 285 eV, C–O/C–N at 286.5 eV, and C=O at 288.3 eV;²⁵ however, it is not significantly dissimilar to the silanol-terminated Si wafer since hydrocarbon contamination also exhibits these functional groups. It must be noted that the highest binding energy carbon peak (labeled as the C–C=O peak) has a large uncertainty as the peak is very small and appears as a shoulder in the spectrum. The binding energy of this peak is 0.9 eV smaller than the respective peak in Figure 2A. However, as the uncertainties of the high binding energy peaks in both Figure 2A and Figure 3A are rather large, no further conclusions can be drawn from this observation. The presence of APTES on the surface was confirmed by the N 1s spectrum (shown in 3B) showing peaks attributable to hydrogen bonded NH₂ at 402.4 eV⁵ and NH₂ terminal groups on APTES that are not hydrogen bonded (“free NH₂”) at 400.9 eV.⁵ These components are expected to be present in the spectrum of a surface that has been successfully modified with APTES.⁵ Table 3, Table 4, and Table 5 provide quantification of the high-resolution spectra in Figure 3.

Table 3. Quantification of the C 1s XP Spectrum in Figure 3A

species	position (eV)	contribution (%)
C–C	285.0	80 ± 1
C–O/C–N	286.5 ± 0.2	17 ± 1
C–C=O	288.3 ± 0.7	3 ± 1

Table 4. Quantification of the N 1s XP Spectrum in Figure 3B

species	position (eV)	contribution (%)
H-bonded NH ₂	402.4 ± 0.2	40 ± 0.5
“free” NH ₂	400.9 ± 0.2	60 ± 0.5

Table 5. Quantification of the Si 2p XP Spectrum in Figure 3C^a

species	position ^b (eV)	contribution (%)
bulk Si	99.1 ± 0.1	51 ± 0.5
oxidized Si	103.8 ± 0.2	49 ± 0.5

^aThe position of the Si 2p 3/2 peak is shown. ^bSi 2p 3/2 peak positions.

Comparing the Si 2p spectrum from the APTES-modified Si surface (Figure 3C) with the Si 2p spectrum from a silanol-terminated Si surface (Figure 2B) reveals that there is an increase in the silicon dioxide peak (103.8 eV) compared to the bulk Si peak (99.1 eV). On the APTES-modified surface the

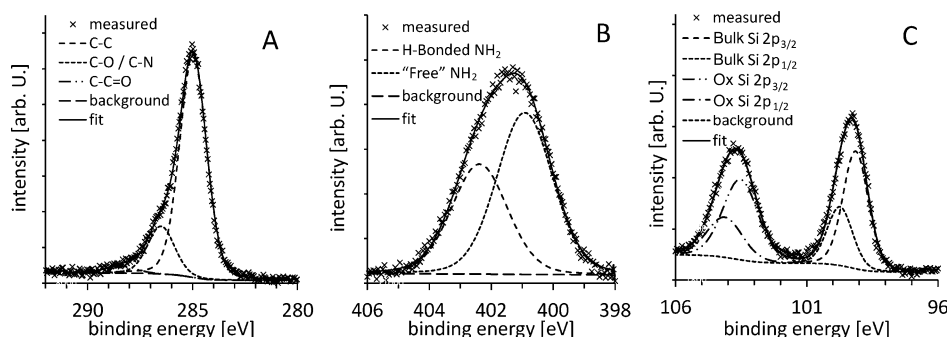


Figure 3. High-resolution XP spectra from APTES-modified Si. (A) C 1s, (B) N 1s, and (C) Si 2p.

ratio of the Si peak to the SiO₂ peak is approximately 50/50, but for the silanol-terminated Si wafer the ratio is 80/20. An increase in the contribution from SiO₂ on the APTES-modified Si surface may occur due to two factors: first, the addition of APTES onto the surface results in a thicker layer on top of the bulk silicon than the silanol termination alone, and this will result in an attenuation of the bulk Si XPS signal due to the limited inelastic mean free path of electrons, i.e., the probe depth of XPS,²⁵ and second that APTES itself contains Si–O bonds.

Table 6 presents the quantification of the peaks in the XP survey spectrum from APTES-modified silicon. It can be seen

Table 6. Survey Spectrum Quantification for APTES-Modified Si

species	relative at. %
C	56 ± 0.5
O	17 ± 0.5
N	4 ± 0.5
Si	23 ± 0.5

from the relative atomic percentages that there is a C:N ratio of 14:1, significantly higher than the 3:1 C:N ratio expected if APTES had perfectly adsorbed in a “tripod structure” with each of the three Si–O groups forming a siloxane bond with silanol-terminated Si wafers. A 14:1 C:N ratio indicates that there are APTES molecules adsorbed to the surface or cross-linked to adsorbed APTES that still retain ethoxy functional groups on some of their Si–O tails, behavior that has been previously observed for APTES.^{2,5,28} The ratio is still higher than the maximum C:N ratio of 9:1 of an unreacted APTES molecule. Repeating the same experiment with a fresh sample yielded the same result.

XPS measurements confirm the successful attachment of APTES to the surface of the silanol-terminated Si wafers. However, the ratio between the nitrogen signal and that of carbon is too small for APTES that has formed three siloxane bonds with the silanol-terminated silicon surface and could be

due to several reasons. The first reason could be the adsorption of a hydrocarbon on the surface or the incorporation of such hydrocarbons into the APTES layer. Toluene is the only compound which is present to a larger extent during the preparation of the APTES layer. Incorporation of toluene into the APTES layer is not considered likely as this compound does not chemically interact with the silanol-terminated silicon or with the APTES. Further, toluene has a large vapor pressure and should readily evaporate after fabrication or when the samples are exposed to vacuum during analysis. If a large amount of toluene was present on the surface, then C 1s XP spectra would be expected to show the presence of an aromatic ring at a binding energy of 284.5 eV, which is not the case as can be seen in Figure 3. Another source for hydrocarbons might be adventitious hydrocarbons contaminating the silanol-terminated silicon. Some of this contamination might not be removed during the adsorption process of the APTES on the silanol-terminated silicon and thus might be left over on the sample surface. The second reason for the high C:N ratio could be that not all ethoxy groups of the APTES react with the silanol terminated silicon surface, thus leaving the ethoxy groups unreacted, leading to a C:N ratio larger than 3:1. The third reason for the high C:N ratio could be that the NH₂ does not terminate the APTES layer but instead is folded into the attached APTES layer. Due to the limited electron mean free path, the nitrogen signal would be attenuated leading to a higher C:N ratio in comparison to an entirely NH₂ group terminated APTES layer. The MIES and UPS measurements give evidence that the second and the third reasons have more foundation than the first. However, as will be shown below, adventitious hydrocarbons remaining from contamination of the silanol-terminated silicon might have to be taken into account.

UPS and MIES Analysis of APTES on a Silanol-Terminated Si Wafer. Figure 4A and Figure 4B show the UP and MIE spectrum of APTES deposited on polycrystalline silver via CVD at 90 K. The UP and MIE spectra shown are the measured spectra after subtracting the secondary electron background. The spectra can be used as reference spectra for

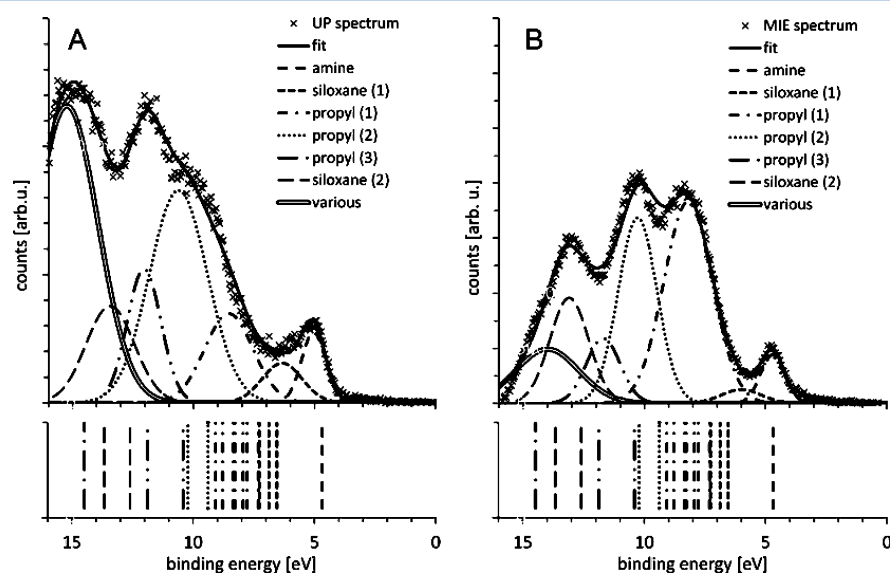
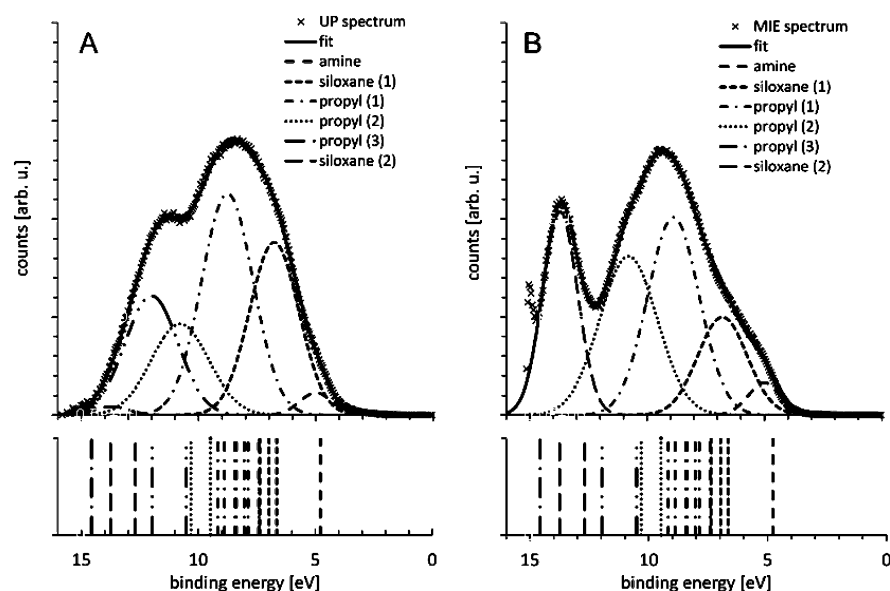


Figure 4. (A) UP and (B) MIE background subtracted spectra of APTES CVD grown on silver at 90 K. Underneath the spectra the calculated positions of DOS are shown.

Table 7. Position, fwhm, and Location of the MOs on the APTES Molecule of the Peaks Fitted to the MIE and UP Spectra of CVD APTES on Silver^a

fitted peak	position of fitted peak [eV]	position relative to amine [eV]	fwhm of fitted peak [eV]	difference in position between fitted and calculated peaks [eV]	MO location
amine	4.8 ± 0.2	-	1.4 ± 0.2	0.4 ± 0.2	NH ₂
siloxane (1)	6.2 ± 0.3	1.4 ± 0.4	2.2 ± 0.3	-0.6 ± 0.3	siloxane
propyl (1)	8.4 ± 0.2	3.6 ± 0.3	2.4 ± 0.1	0.3 ± 0.3	propyl chain
propyl (2)	10.5 ± 0.2	5.7 ± 0.3	2.8 ± 0.1	0.8 ± 0.2	propyl chain
propyl (3)	11.9 ± 0.2	7.1 ± 0.3	2.1 ± 0.5	0.9 ± 0.2	propyl chain
siloxane (2)	13.3 ± 0.2	8.5 ± 0.3	2.1 ± 0.3	0.3 ± 0.2	siloxane

^aAlso the difference in position between the fitted peak and the calculated DOS is shown. For the DOS, the average position of the DOS covered by a single fitted peak is given. The fitted and calculated peak positions differ by up to 0.6 eV for most of the peaks. Given that the fwhm is much larger than this difference, the agreement between calculated and fitted peak position may be considered as acceptable for the purpose of identifying the nature of the peaks. Only for the peaks “propyl (2)” and “propyl (3)” is a larger difference observed, 0.8 and 0.9 eV, respectively. The reason for this larger difference is most likely that in this binding energy range it is more difficult to localize the MOs unambiguously on the molecules due to orbital intermixing.

**Figure 5.** (A) UP and (B) MIE background subtracted spectra of APTES-modified Si. Underneath the spectra the calculated positions of DOS are shown. They are identical to those shown in Figure 4.

APTES as the sample consists only of APTES. The presence of impurities can be excluded as the liquid APTES used for the CVD process was degassed and no impurities were present in the UHV chamber, as confirmed by residual gas analysis of the chamber prior to the measurement.

Both measured spectra could be fitted well with a set of 7 Gaussian curves plus an exponential curve for the secondary electron background. To relate each of the peaks to the respective functional group of APTES, the binding energy of the peaks was compared with the DOS calculations. This was done for both NH₂(CH₂)₃Si(OH)₃ as well as the full APTES molecule (NH₂(CH₂)₃Si(O(CH₂)CH₃)₃) since the former represents the molecule formed in the silanization reaction. Both calculations show that in the region of binding energy up to 12 eV the only difference between the two molecules is that in the range representing the siloxane group a larger number of states can be found for the full APTES molecule but still at similar binding energies. Thus, using either of the molecules for calculating a reference for the DOS leads to the same result of the analysis.

In Figure 4A and Figure 4B the molecular orbitals (MOs) with the binding energy, as determined through the DOS

calculations, are shown as vertical lines in the lower panel. As described in the Experimental Section, in the process of identifying the peaks in the measured spectra, shifting of the position of the calculated DOS along the binding energy scale relative to the fitted peaks was allowed by adding the same offset to all MOs and thus keeping the relative position of the calculated MOs constant.

The MO with the lowest binding energy is located on the NH₂ group, forming a clear peak at 4.8 eV. At 6.2 eV the MOs located on the siloxane group can be found followed by the MOs on the propyl chain at 8.4 and 10.5 eV. All these features appear clearly in both the UP and the MIE spectra. It has to be noted that the peak due to the siloxane group at 6.0 eV is located at a minimum in both the UP and the MIE spectra, and the exact position of the fitted peak has a much larger degree of uncertainty than the other peaks. At 11.9 eV a peak can be identified in the UP spectrum that can be attributed to the MOs on the propyl chain. This peak cannot clearly be seen in the MIE spectrum. At this binding energy, the secondary electron background starts to dominate both the UP and the MIE spectra. It is also difficult to unambiguously identify the position of the subsequent peak at 13.7 eV (dominated by MOs

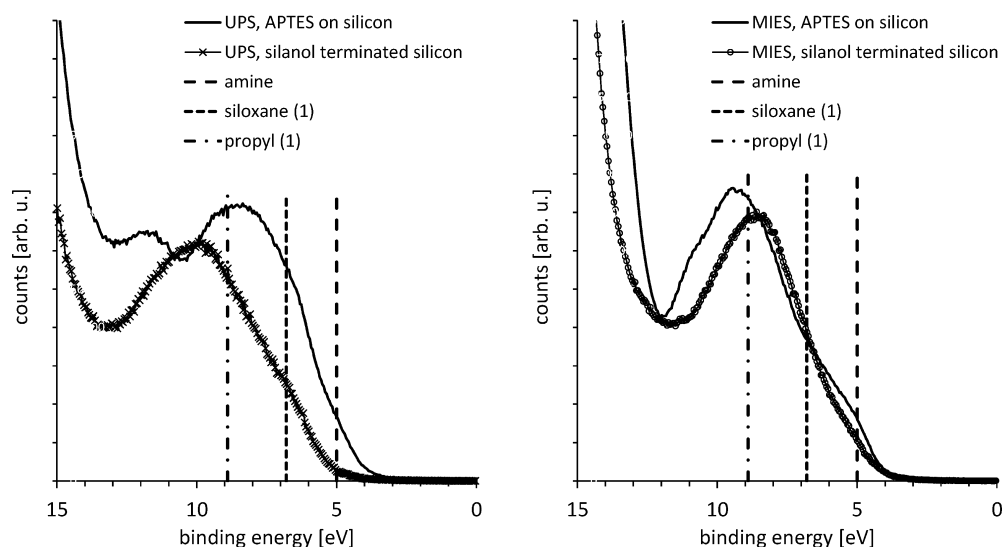


Figure 6. Comparison between the UP and MIE spectra of the silanol-terminated silicon and the APTES-modified silicon. The secondary electron background has not been removed from the spectra in this figure as for the purpose of comparison the spectra do not need to be fitted with peaks (as in Figure 4 and Figure 5). The position of the amine, siloxane (1), and propyl (1) is indicated with vertical lines.

on the siloxane group) and the peak at 15 eV. The assignment of the MOs together with their position and the fwhm of the fitted peaks is summarized in Table 7. All fitted peaks, apart from that of amine, represent more than a single DOS as can be seen in Figure 4. It must be noted that the fitted peaks covering more than a single DOS are broader than the peak representing a single DOS.

The UP spectrum of the APTES-modified Si surface is shown in Figure 5A and the MIE spectrum in Figure 5B. Most of the peaks can be identified in these spectra as in the spectra shown in Figure 4. In Figure 5, the positions of the fitted peaks labeled “amine”, “siloxane (1)”, “propyl (1)”, and “propyl (2)” are the same as those in Figure 4 (within an uncertainty of 0.2 eV). The peaks “propyl (3)”, “siloxane (1)”, and “various” do not appear clearly in the UP and the MIE spectra due to a larger secondary electron background of the spectra in Figure 5 compared to that in Figure 4. For this reason the three peaks at the higher binding energy are much harder to fit with high certainty and cannot be clearly separated from the secondary electron background. This has no significant influence on the analysis as these peaks do not need to be considered further in the discussion.

Understanding of the formation process and structure of the APTES can be gained by comparing the peak intensities of the UP spectra in Figure 4 and Figure 5 and the MIE spectra in these two figures. This comparison focuses on the peaks due to the MO of the NH_2 at 5.0 eV, the MOs located on the siloxane group at 6.8 eV, and the MOs on the propyl chain at 8.8 eV. In the binding energy range of these peaks, the spectra are only slightly affected by the secondary electron background, and the peak intensities can be compared. The position of the propyl chain peak relative to that of NH_2 is 3.8 ± 0.3 eV and almost the same as for the spectra of APTES on silver. The position of the siloxane peak relative to that of NH_2 is 1.8 ± 0.3 eV and somewhat larger than in the spectra of APTES on silver. In the latter case, the difference in relative peak position seems to be significant. However, it was noted above that the position of the fitted peak due to the siloxane group in the spectrum of the APTES on silver has a high degree of uncertainty.

Comparing the three selected peaks, i.e., those of the NH_2 , the siloxane group, and the propyl chain, in the spectra of APTES on silver and the APTES-modified silicon, it can be seen that the siloxane group peak shows a much higher intensity in the latter. This difference between the spectra can be attributed to either the presence of a compound other than APTES or differences in the structure between the CVD APTES layers and the APTES layer attached to the silicon substrate through the surface reaction. The only compound other than APTES that could be present in the film is toluene. DOS calculation of toluene has been performed, and the results are very close to those reported in refs 29 and 30. According to the DOS calculation, the MO with the lowest binding energy in toluene is at a binding energy similar to that on the siloxane group of APTES at 6.8 eV. In the discussion of the XPS results, it was concluded that the presence of a considerable amount of toluene in the APTES film is unlikely. Thus, the differences between the spectra in Figure 4 and Figure 5 are attributed to differences in the structure of the APTES layers.

For the interpretation of the differences in the spectra between the APTES-modified surface and the CVD APTES sample, it has to be taken into account that MIE probes exclusively the outermost layer. UPS probes the surface near region up to a depth of a few nanometers, and the contribution of emitted electrons to the spectrum decreases exponentially with the depth since it is controlled by the electron mean free path. An increase in intensity of a peak in the MIE spectrum means that more of the outermost layer consists of the respective functional group. An increase in intensity in the UP spectrum is a strong indication that the respective group is closer to the outermost layer. Yet some of the signal changes observed may also be due to molecular reorientation as well as an altered local molecular environment. This will affect both the angular emission direction and even the photoionization cross section, thus no conclusions are drawn from the fact that the relative intensities in the UP spectra change between Figure 4 and Figure 5.

In both the UP and the MIE spectra, a higher intensity of the MO of the siloxane group compared to the MO of the NH_2 group and the lowest binding energy MO on the propyl chain

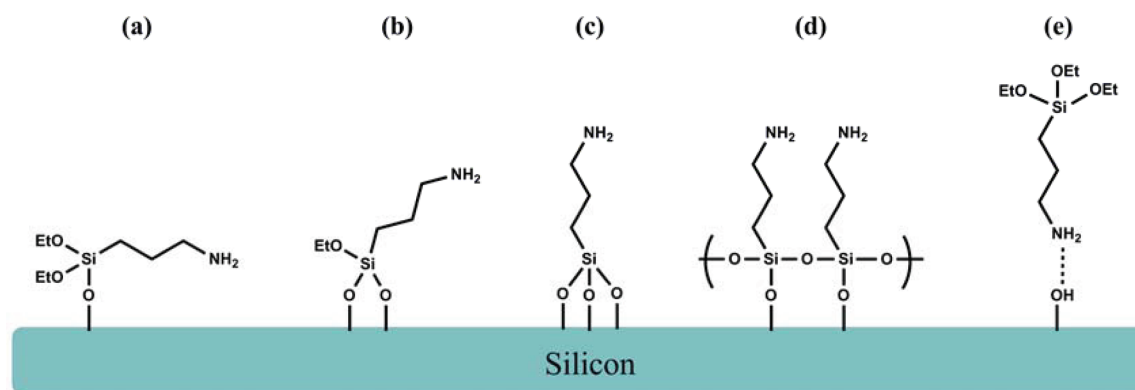


Figure 7. Possible orientation of the APTES molecule attached to the silanol-terminated silicon surface through the silanization reaction. Further, it cannot be ruled out that residual hydrocarbon impurities are incorporated into the APTES layer.

in the spectrum of the APTES-modified Si is found. This allows for two conclusions: first, the siloxane group is close to the outermost layer in the APTES-modified Si and covers more of this layer. Second, the molecules in the layer of APTES on silver must be oriented differently than in the APTES layer attached to the silicon surface. Thus, the structure of the APTES layer on silicon is different from that sketched in Figure 1. Instead, a combination of possible orientations like those sketched in Figure 7 are the likely result of the silanization reaction: reaction of only one (a) or two (b) of the ethoxy groups with the silanol-terminated silicon, reaction of all three ethoxy groups with the silanol-terminated silicon (c), cross-linking of the APTES molecules (d), or attachment of the NH₂ group of the APTES molecule to the surface (e). The formation of --NH--Si can be excluded as in this case the nitrogen signal would be found approximately at 397 eV in the XP spectrum,³¹ whereas Figure 3B and Table 3 only show a nitrogen contribution at 400.9 and 402.4 eV.

As the peak intensities strongly differ between both samples, it is likely that the siloxane group is pointing toward the substrate in the case of the CVD APTES layer and thus that the outermost layer is dominated by the NH₂ group in this case.

A consequence of this finding is that on the APTES-modified surface only a small fraction of the surface is terminated by the NH₂ group and available for further chemical reactions.

Apart from the orientation of the adsorbed APTES molecules, hydrocarbon impurities of the silanol-terminated silicon surface remaining after the APTES modification could influence the UP and MIE spectra in Figure 5. In Figure 6, the UP and MIE spectra of the silanol-terminated silicon and the APTES-modified silicon are compared. It can be seen that at the amine position the hydrocarbon impurities show only a minor contribution to the spectra, but at the siloxane (1) and propyl (1) position a considerable contribution to the spectra can be found. The consequence is that residual hydrocarbon impurities cannot be ruled out on the silanol-terminated silicon surface after the APTES modification.

CONCLUSION

The modification of a silanol-terminated silicon surface after a silanization reaction with APTES has been investigated. Reference spectra of APTES adsorbed on polycrystalline silver through a CVD process and DOS calculations have been used to identify the contributions in the spectrum of the APTES-modified Si surface. XPS has confirmed the formation of the APTES layer. The comparison of the UP and MIE spectra of

APTES adsorbed on polycrystalline silver and the APTES-modified Si surface shows that APTES reacts only partially with the silanol-terminated silicon surface but also undergoes a polymerization reaction cross-linking the APTES molecules. Further, it cannot be ruled out that residual hydrocarbon impurities are incorporated into the APTES layer. As a consequence, the APTES layer formed shows a strong presence of siloxane groups close to the surface of the APTES layer formed and a lack of the presence of NH₂ groups. This has implications for the ability of the APTES layer to function as a coupling agent for further reactions via the NH₂ group. A variation of the reaction conditions for reacting APTES with the silanol-terminated Si surface might lead to a higher fraction of the APTES layer being terminated with the NH₂ group.

AUTHOR INFORMATION

Corresponding Author

*E-mail: gunther.andersson@flinders.edu.au.

Notes

The authors declare no competing financial interest.

ACKNOWLEDGMENTS

This project was supported by Queensland State Government Smart State National and International Research Alliances Program (NIRAP). We would like to thank eResearchSA for the use of their high-performance computational facilities and support.

REFERENCES

- (1) Kim, J.; Cho, J.; Seidler, P. M.; Kurland, N. E.; Yadavalli, V. K. *Langmuir* **2010**, *26*, 2599.
- (2) Pasternack, R. M.; Rivillon Amy, S.; Chabal, Y. J. *Langmuir* **2008**, *24*, 12963.
- (3) Qin, M.; Hou, S.; Wang, L.; Feng, X.; Wang, R.; Yang, Y.; Wang, C.; Yu, L.; Shao, B.; Qiao, M. *Colloids Surf., B* **2007**, *60*, 243.
- (4) Chiang, C.-H.; Liu, N.-I.; Koenig, J. L. *J. Colloid Interface Sci.* **1982**, *86*, 26.
- (5) Vandenberg, E. T.; Bertilsson, L.; Liedberg, B.; Uvdal, K.; Erlandsson, R.; Elwing, H.; Lundström, I. *J. Colloid Interface Sci.* **1991**, *147*, 103.
- (6) Vaidya, A. A.; Norton, M. L. *Langmuir* **2004**, *20*, 11100.
- (7) Lin, C.-H.; Hung, C.-H.; Hsiao, C.-Y.; Lin, H.-C.; Ko, F.-H.; Yang, Y.-S. *Biosens. Bioelectron.* **2009**, *24*, 3019.
- (8) Moiseev, L.; Ünlü, M. S.; Swan, A. K.; Goldberg, B. B.; Cantor, C. R. *Proc. Natl. Acad. Sci. U.S.A.* **2006**, *103*, 2623.
- (9) Rathor, N.; Panda, S. *Mater. Sci. Eng.: C* **2009**, *29*, 2340.

- (10) Zhao, J.; Li, Y.; Guo, H.; Gao, L. *Chin. J. Anal. Chem.* **2006**, *34*, 1235.
- (11) Han, Y.; Mayer, D.; Offenhäusser, A.; Ingebrandt, S. *Thin Solid Films* **2006**, *510*, 175.
- (12) Wang, L.; Feng, X.; Hou, S.; Chan, Q.; Qin, M. *Surf. Interface Anal.* **2006**, *38*, 44.
- (13) Herlem, G.; Segut, O.; Antoniou, A.; Achilleos, C.; Dupont, D.; Blondeau-Patissier, V.; Gharbi, T. *Surf. Coat. Technol.* **2008**, *202*, 1437.
- (14) Morgner, H. *Adv. At., Mol. Opt. Phys.* **2000**, *42*, 387.
- (15) Voigts, F.; Bebensee, F.; Dahle, S.; Volgmann, K.; Maus-Friedrichs, W. *Surf. Sci.* **2009**, *603*, 40.
- (16) Heinz, B.; Morgner, H. *Surf. Sci.* **1997**, *372*, 100.
- (17) Ito, E.; Yamamoto, M.; Kajikawa, K.; Yamashita, D.; Ishii, H.; Ouchi, Y.; Seki, K.; Okawa, H.; Hashimoto, K. *Langmuir* **2001**, *17*, 4282.
- (18) Maus-Friedrichs, W.; Frerichs, M.; Gunhold, A.; Krischok, S.; Kempter, V.; Bihlmayer, G. *Surf. Sci.* **2002**, *515*, 499.
- (19) Gunster, J.; Kempter, V.; Souda, R. *J. Phys. Chem. B* **2005**, *109*, 17169.
- (20) Shirley, D. A. *Phys. Rev. B* **1972**, *5*, 4709.
- (21) Oberbrodthage, J. *J. Electron Spectrosc. Relat. Phenom.* **1998**, *95*, 171.
- (22) Li, X.; Zhang, Z.; Henrich, V. E. *J. Electron Spectrosc. Relat. Phenom.* **1993**, *63*, 253.
- (23) Seah, M. P.; Dench, W. A. *Surf. Interface Anal.* **1979**, *1*, 2.
- (24) Frisch, M. J.; Trucks, G. W.; Schlegel, H. B.; Scuseria, G. E.; Robb, M. A.; Cheeseman, J. R.; Scalmani, G.; Barone, V.; Mennucci, B.; Petersson, G. A.; Nakatsuji, H.; Caricato, M.; Li, X.; Hratchian, H. P.; Izmaylov, A. F.; Bloino, J.; Zheng, G.; Sonnenberg, J. L.; Hada, M.; Ehara, M.; Toyota, K.; Fukuda, R.; Hasegawa, J.; Ishida, M.; Nakajima, T.; Honda, Y.; Kitao, O.; Nakai, H.; Vreven, T.; Montgomery, Jr., J. A.; Peralta, J. E.; Ogliaro, F.; Bearpark, M.; Heyd, J. J.; Brothers, E.; Kudin, K. N.; Staroverov, V. N.; Kobayashi, R.; Normand, J.; Raghavachari, K.; Rendell, A.; Burant, J. C.; Iyengar, S. S.; Tomasi, J.; Cossi, M.; Rega, N.; Millam, N. J.; Klene, M.; Knox, J. E.; Cross, J. B.; Bakken, V.; Adamo, C.; Jaramillo, J.; Gomperts, R.; Stratmann, R. E.; Yazyev, O.; Austin, A. J.; Cammi, R.; Pomelli, C.; Ochterski, J. W.; Martin, R. L.; Morokuma, K.; Zakrzewski, V. G.; Voth, G. A.; Salvador, P.; Dannenberg, J. J.; Dapprich, S.; Daniels, A. D.; Farkas, Ö.; Foresman, J. B.; Ortiz, J. V.; Cioslowski, J.; Fox, D. J. *Gaussian 09*, revision B.01; Gaussian, Inc.: Wallingford, CT, 2009.
- (25) O'Boyle, N. M.; Tenderholt, A. L.; Langner, K. M. *J. Comput. Chem.* **2008**, *29*, 839.
- (26) Keller, W.; Morgner, H.; Müller, W. A. *Mol. Phys.* **1986**, *57*, 623.
- (27) Briggs, D.; Seah, M. P. *Practical surface analysis*, 2nd ed.; Wiley: Chichester; New York; Aarau, 1990; Vol. 1.
- (28) Arranz, A.; Palacio, C.; García-Fresnadillo, D.; Orellana, G.; Navarro, A.; Muñoz, E. *Langmuir* **2008**, *24*, 8667.
- (29) Kimura, K.; Katsumata, S.; Achiba, Y.; Yamazaki, T.; Iwata, S. *Handbook of HeI Photoelectron Spectra of Fundamental Organic Molecules*; Japan Scientific Societies Press: Tokyo, 1981.
- (30) Ananthavel, S. P.; Ganguly, B.; Chandrasekhar, J.; Hegde, M. S.; Rao, C. N. R. *Chem. Phys. Lett.* **1994**, *217*, 101.
- (31) Choukurov, A.; Grinevich, A.; Hanuš, J.; Kousal, J.; Slavínská, D.; Biederman, H.; Bowers, A.; Hanley, L. *Thin Solid Films* **2006**, *502*, 40.